Journal of Applied Fluid Mechanics, Vol. 17, No. 7, pp. 1499-1513, 2024.
Available online at www.jafmonline.net, ISSN 1735-3572, EISSN 1735-3645.
https://doi.org/10.47176/jafm.17.7.2360

Investigating Pressure Gradient Dynamics in Two-phase Fluid Flow through Porous Media: An Experimental and Numerical Analysis

H. Ashouri[1], H. Mohammadiun[1†], M. Mohammadiun[1], G. Shafiee Sabet[1], M. H. Dibaee Bonab[1] and F. Sabbaghzadeh[2]

[1] *Department of Mechanical Engineering, Shahrood Branch, Islamic Azad University, Shahrood, Iran*
[2]*Department of Chemical Engineering, Shahrood Branch, Islamic Azad University, Shahrood, Iran*

†*Corresponding authorshmohammadiun@iau-shahrood.ac.ir*

ABSTRACT

This study investigates pressure gradient dynamics within a porous medium in the context of two-phase fluid flow, specifically water and sand particle interactions. Using experimental data, we refine pressure correction coefficients within a numerical solution framework, employing the Semi-Implicit Method for the Pressure-linked Equations algorithm. Our findings highlight the relative nature of pressure gradient phenomena, with particle size and volume fraction emerging as crucial determinants. Graphical representations reveal a clear trend: an increase in volume fraction, up to 40%, across varying Reynolds Numbers, leads to a transition towards non-Newtonian behavior in the two-phase fluid system. Unlike the linear pressure gradient seen in single-phase fluid flow, the interplay between liquid and solid phases, along with drag forces, imparts a distinctly nonlinear trajectory to the pressure gradient in two-phase fluid flow scenarios. As the two-phase flow enters a porous medium, numerous factors come into play, resulting in a pressure drop. These factors include changes in cross-sectional geometry, alterations in boundary layer dynamics, and ensuing momentum fluctuations. Interestingly, an increase in porosity percentage inversely correlates with pressure gradient, resulting in reduced pressure gradient with higher porosity levels.

Article History

Received October 10, 2023
Revised January 7, 2024
Accepted February 3, 2024
Available online April 30, 2024

Keywords:

Two-phase fluid flow
Porous media
Interaction
Pressure gradient
Porosity percentage

1. INTRODUCTION

The porous medium numerically define within the framework of the Darcy model in our discussions. This model is constructed based on pressure drop and alterations within the porous medium. The pores may exist on its surface or within its internal structure. The concept of porosity relates to the density of the material and its constituents. In numerical simulations, the empty spaces within the medium can liken to a mobile phase, wherein the porous medium is treated as a mobile region using numerical methods. To explore pressure gradients in porous media and their impact on parameters such as flow rate and porous structure, it is advantageous to redefine the porous medium as a composite of solid and fluid phases.

Multiphasic fluid flows entail the movement of solid particles within liquids or gases, droplets in gases, bubbles in liquids, or a combination thereof. In such flows, the particles are typically called the second phase. The flow within an encompassing medium is termed the first phase. Understanding the dynamics of two-phase fluid flows is a profoundly intricate endeavor, given its challenges in dealing with boundary conditions, interfaces, momentum, heat transfer, mass, and intra-phase reactions.

Within a porous medium, the contact surface area between the fluid and the solid body is exceptionally high. This characteristic significantly contributes to reducing the thermal inertia of heat exchangers. Consequently, researchers have consistently favored using porous media in heat exchangers (Bear, 1948; Chen 2009; & Arasteh et al. 2019)

Arasteh et al. (2019) conducted a study using sinusoidal waves to assess the impact of metal foam porous media on heat transfer and fluid mechanics within heat exchangers. This investigation involved various geometries and distance ratios, ultimately revealing that porous media significantly enhance heat transfer while sinusoidal geometry has a substantial effect on pressure drop.

Alomar et al. (2020) delved into numerous parameters, including Reynolds numbers and pressure drops, in a numerical examination of two-phase flows

NOMENCLATURE

u	standard uncertainty	hPa	hectopascal
a	device precision	C	centigrade
y	input function	$mmH2O$	millimeter of water
U	uncertainty expanded	FVM	Finite Volume Method
p	pump power	DPM	Discreet Phase Method
I	pump Ampere	CFD	Computerized Fluid Dynamic
V	pump Voltage	x_i	uncertainty
$u(y)$	uncertainty of the measurand y	δ	device accuracy
$u(xi)$	number of measurements xi	$power$	power
$multi$	multimeter	$current$	current
$Volt$	voltage		

within heat exchangers filled with porous media. The findings indicated that the properties of the porous medium have a negligible effect on heat transfer but can be influential when the Reynolds number of the inlet flow is low. The Incorporation of porous media in two-phase flows can enhance heat transfer.

Also, in (2020), Naqvi and Wang (2020) explored the effect of porous media on heat transfer and fluid mechanics by deploying porous media to dampen baffle vibrations within a loose heat exchanger and tube assembly. The utilization of porous media not only reduced baffle vibrations by absorbing the vortices generated by baffles but also played a pivotal role in enhancing heat transfer, consequently prolonging the converter's lifespan.

Siavashi and Joibary (2019) examined the influence of nanofluid and porous media on heat transfer through a numerical investigation of a two-tube cross-current heat exchanger. Their results demonstrated a direct relationship between Darcy and Reynolds numbers and nanofluid properties. Moreover, they highlighted the significant role of porous media in enhancing heat transfer.

Shirvan et al. (2016) numerically studied a two-tube heat exchanger filled with porous media. Their research shed light on the impact of variations in Reynolds and Darcy numbers on heat transfer within the exchanger. Sensitivity analysis and numerical investigations across different Reynolds number ranges revealed that the thermal behavior of the heat exchanger filled with porous media is contingent upon the Reynolds number's magnitude. The study also affirmed the positive influence of porous media on the efficiency of the two-tube heat exchanger. The utilization of porous media in heat exchangers, owing to its ability to increase surface area and favorable ductility, has captivated the interest of researchers across diverse applications. This has led to the development of a broad spectrum of knowledge about to the use of porous media.

Mellouli et al. (2009) studied hydrogen storage within a heat exchanger filled with porous metal media. Their research revealed the positive impact of utilizing porous media on hydrogen storage. By performing numerical analyses on a heat exchanger with metal foam replacing traditional media, they demonstrated that this substitution significantly increased the hydrogen storage process. Furthermore, the duration for which hydrogen could be retained in the tank increased by an impressive 90% compared to conditions without foam. Flow rate is a critical parameter in determining the efficiency of heat exchangers. Increasing the Reynolds Number of flow within the heat exchanger simultaneously boosts the net heat transfer rate and induces pressure drop.

Joibary and Siavashi (2019) investigated a two-tube heat exchanger employing porous media to examine the Reynolds Number's impact on efficiency. Their findings indicated that using porous media can influence heat transfer rates. Interestingly, they observed that the optimal mode for this heat exchanger decreased compared to conventional conditions, attributed to the presence of porous media. This speed reduction, however, was associated with an increase in heat transfer efficiency.

Zhang & Tahmasebi (2019) explored the effect of particle size on the deformation of porous media. They established a direct relationship between particle size and pressure changes, as well as other flow parameters within porous media. Their study also confirmed that mathematical and computational models based on dry and wet porous media behaved effectively and exhibited good predictive capabilities.

Moving to 2023, several researchers made significant contributions to the understanding of multiphase flows in porous media. Roman (2023) proposed a dual model for the location of two-phase flow within porous media while examining disturbances throughout the enclosed area. They illustrated the trends in pressure changes caused by the pressure gradient. Man et al. (2023) developed a model for intermittent convection drying using multiphase flow within porous media, incorporating Darcy's law and gradient changes in pressure. They examined capillary effects. Tammisola (2023) focused on multiphase viscoelastic and elastoviscoplastic fluid flows, presenting dimensionless time-averaged pressure gradients as a function illustrating non-uniform pressure drops. Jiang et al. (2023) demonstrated that capillary-guided two-phase flow within porous media induced movement and separation of gas phases due to pressure gradients. Zheng et al. (2023) highlighted the significance of porous striations perpendicular to the flow direction in two-phase flow and pressure gradients within porous media.

In this vein, Sharma et al. (2023) investigated immiscible two-phase flows in porous media, emphasizing that high-pressure gradients generated by emulsions overcame capillary force trapping. Liang et al. (2023) explored fluid replacement within porous media, illustrating how forces and multiphase flow interfaces led to relatively uniform pressure gradients. Chen et al.

(2023a) revealed a proportional relationship between material diffusion speed gradients within porous media and pressure gradients, depending on the material type. Tounsi et al. (2023) examined the flow of saltwater through deformed porous media, highlighting that convective fluid flow was induced solely by pressure gradients. Finally, Chen et al. (2023b) developed a visual and effective method to study multiphase flow within porous media, showing that injecting a solution could create a higher excess pressure gradient.

Akram et al. (2022) investigated the effects of concentration and nanoparticle sliding parameters on solvent concentration and nanoparticle fraction. They observed increased velocity at the center of the channel with higher velocity slip coefficients, while the opposite behavior occurred at the channel walls. Similarly, Saeed et al. (2022) explored the impact of sliding boundaries on velocity, heat, and concentration convection within a magnetic tangent hyperbolic nanofluid subject to peristaltic flow. They mathematically defined the equations governing the tangential magnetic hyperbolic nanofluid flow and solved them using numerical techniques. Their study also emphasized the importance of physical parameters such as Soret and Dufour diffusion parameters, Hartmann number, thermophoresis parameter, power law index, and Brownian motion. Janfada et al. (2022) investigated a direct contact vapor distillation model in soil. in this The porous medium was analyzed by using the direct method in the current porous media model, and the pressure gradient Similarly in 2022 Hasanzadeh et al. (2022) experimentally investigated the pressure gradient of the two-phase flow of water and oil with very high viscosity in a horizontal pipe. The values of the pressure gradient obtained with the predicted values were compared and the results showed that the values are in good agreement with each other.

To investigate particle in porous media and its effect on pressure drop parameter, it is necessary to redefine the porous medium as a mixture of solid and fluid phases. As a result of a combined heuristic solid and fluid phase, a two-phase area from the solid porous medium of open cells and a fluid area within the solid medium, defined as random and multiple internal channels in the medium, are assumed. Simultaneous use of a solid porous medium and a fluid flow within the porous medium improves accuracy and helps determine the fluid's local behavior. It's worth noting that this one-of-a-kind medium for resolving this issue has been precisely defined. The solid particles are trapped in the fluid area before being deposited in the solid phase and change the pressure. Using the Fluent software that is based the Navier-Stock equations and carrying out the discretizing with the methods of CFD plus change from CPU to GPU for solving.

In generally speaking CFD method is based on the discretization of the continuity and momentum equations in three directions. The CFD method is performed, firstly, the geometry describing the flow domain is drawn by considering interacting solid parts with fluids. Secondly, the numerical network is created by separating the fluid domain into the small cells (mesh). The other step is to define the initial and boundary conditions. Finally, the numerical model is run by means of a solver. Post-processing is performed to visualize the findings. CFD discretization methods use Finite Volume (FVM) to their flexibility in creating structured and unstructured meshes for a domain. Mesh structure and mesh quality are directly related to error estimations. A fine mesh structure and the quantity of mesh are so crucial to solving free surface and turbulence effect for reaching a more accurate solution. In this study Discrete Phase Model (DPM) is a multiphase model used to investigation particle injection and tracking and so on. CFD simulation coupled with a DPM has enabled a study to be undertaken of a simplified and repeatable process.

Multiphase system is one characterized by the simultaneous presence of several phases, the two-phase system being the simplest case. The term 'two-component' is sometimes used to describe flows in which the phases consist of different chemical substances. In this study as mentioned in the abstract, the sand and water interaction is multiphase in the other word two- phase fluid flow under investigation. The size of the sands are 5-150 micron and water in normal condition. One of the noteworthy accomplishments of this research is the numerical analysis of liquid-solid fluid flow, specifically focusing on the study of pressure gradients resulting from the intricate interactions between two-phase fluid flows within porous media. To ensure the highest level of numerical solution accuracy, we harnessed the capabilities of ANSYS FLUENT+UDF software, aligning the numerical simulations with the exact geometry of the system.

A key innovation in this work lies in exploring micro-scaled particle movement within the system. Tracking these particles in a numerical context necessitates the utilization of an adaptive network capable of accurately monitoring their trajectories and discerning their influence on fluid behavior. Moreover, integrating porous media and two-phase fluid dynamics has enabled us to employ multilayer networks, using an innovative approach involving mesh birth and death techniques to tackle the complexities of our research problem. In the other word the fineness of the network exists only around the particles in the base fluid, and with the movement of the particles of this active network, it also provides the possibility of generating and erasing the previous networks based on the change of particle location. The criterion for using the Reynolds number is to show the effect of the relationship between velocity and pressure in the turbulence state and the effect it has on the pressure gradient. By considering the solid phase of particles added to the base fluid in various concentrations, the two-phase approach for defining and analyzing micro particles enables the definition of novel concepts in the two-phase media of microstructure.

2. EXPERIMENTAL SECTION

In the realm of experimental testing, it is customary to categorize results into dependent and independent variables. Independent variables are those parameters that

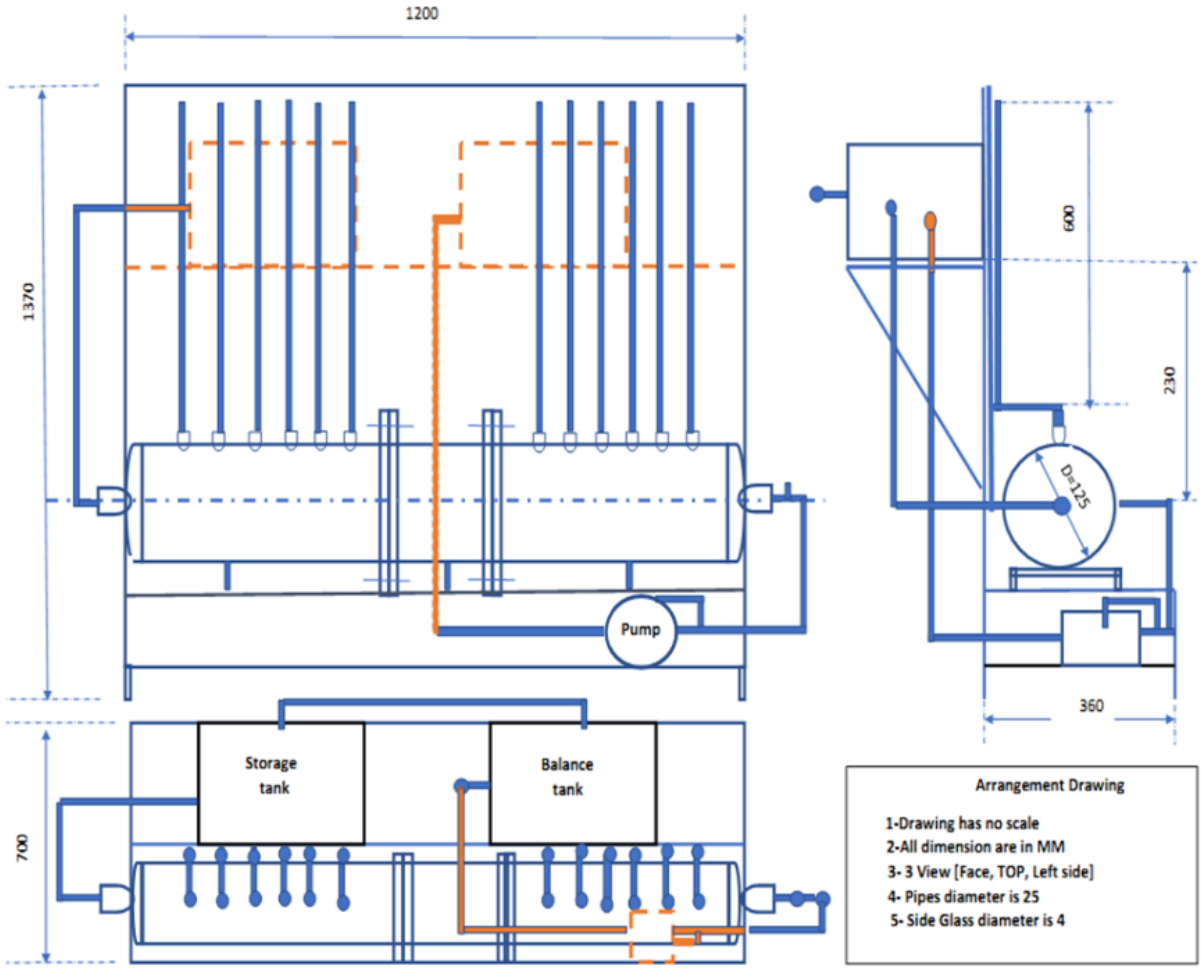

(a)

(b) (c)

Fig. 1 a) Device Arrangement Sketch b) Device Inlet Orientation c) Device Front View

can be quantitatively and accurately measured. In this context, we consider temperature, pressure, velocity, and viscosity as distinct independent parameters. The task of measuring devices is to capture these independent parameters precisely.

Dependent parameters, on the other hand, are functions or outcomes that depend on the variations in independent parameters. These include the Nusselt number, Prandtl number, Reynolds number, heat transfer coefficient, and fluid friction coefficient, to name a few.

In the scope of our research, we meticulously designed and fabricated laboratory equipment following engineering drawings numbered 1 through 3. The experimental tests conduct in two distinct stages, primarily focusing on determining the coefficients of pressure correction. These coefficients were subsequently integrated into the numerical analysis phase of our study.

Figure 2 is actually the set-up made for the experimental test, the important parts of which are shown in Table 1, and the vital part of the device is shown in

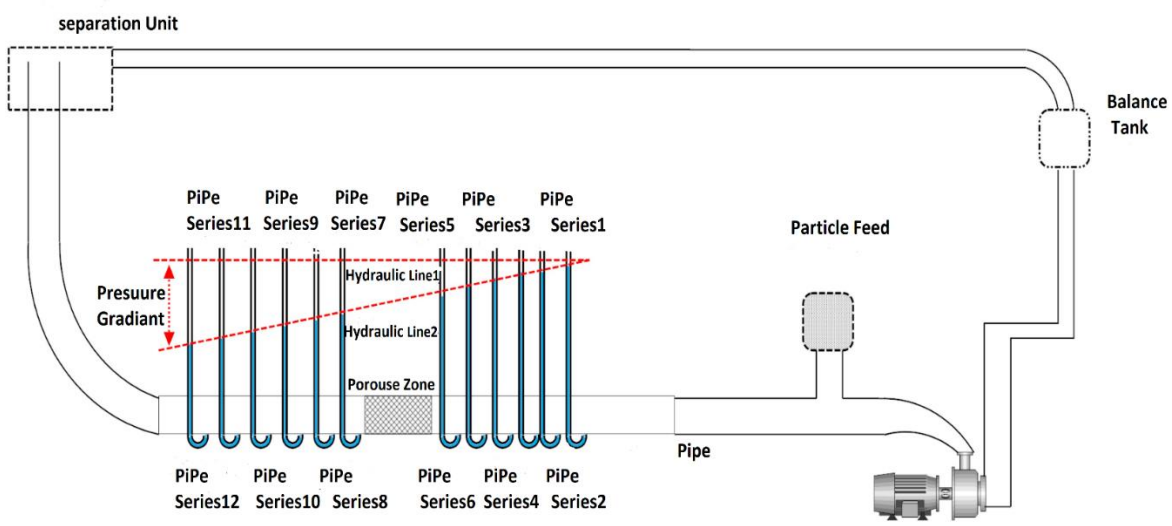

Fig. 2 Equipment layout

Table 1 Equipment Specifications

Dimensions	Range	Material	Equipment
[l/min]	5-36	SQB60	Pump
12pieces D=5[MM]	0-500	Plastic glass	Barometric
15 Liter	100%	Steel	Storage Tank
10 Liter	0-100%	Plastic	Balance tank
25[MM]	100%	Polyethylene	PE-Pipe
12 Pieces	0-100%	Gas Valve ½	globe valve
D=125, l=900 [MM]	0-100%	Seamless steel	steel pipe
D=125, L=200[MM]	0-100%	Seamless steel	prose housing
D=25, L=150[MM]	--	Polyethylene	Nipple

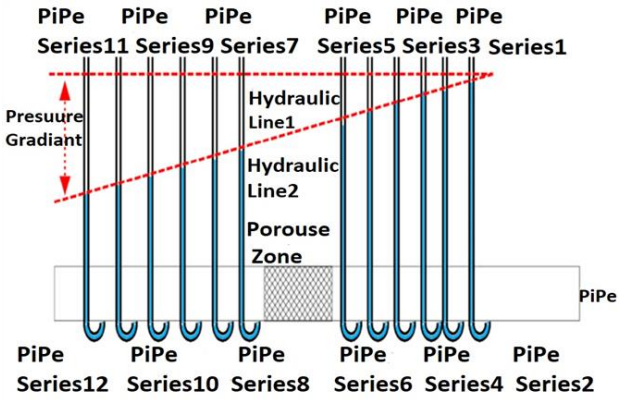

Fig. 3 Examined device section

Fig. 3. And also Fig. 3 shows the location of the study. In the middle part of the figure is the prose media and on the sides of the barometric hoses to measure the pressure data in the experimental mode for use in the numerical analysis. As depicted in Fig. 4, the engineered porous medium was constructed with uniformly sized spherical connections. Engineered porous blade by casting, turning methods and a sample has been designed and made with a 3D printer, and the percentage of porosity is 35.35, although the purpose of this research is to find the effects of porosity in single-phase fluid and two-phase fluid, and the obtained results indicate significant changes in the pressure gradient, which is shown in the graphs.

3. TESTING PROCEDURE

The testing procedure was conducted with precision and adherence to rigorous standards. Here's an overview of the critical steps:

1. Multimeter Calibration: The multimeter used in the experiments was calibrated and certified to ensure accurate measurements.

2. Flow Rate Calculation: The power of the water pump was measured using the multimeter. From this power measurement, the flow rate was calculated. The tube geometry was employed to calculate the velocity of the fluid.

3. Pressure Calculation: Utilizing the obtained velocity in the Bernoulli equation, the pressure within the system was calculated. This analytical pressure data was recorded and rigorously validated.

4. Comparison with Initial Pressure: The calculated pressure was compared with the initial pressure measurements. This comparison served as a critical input for the subsequent numerical analysis.

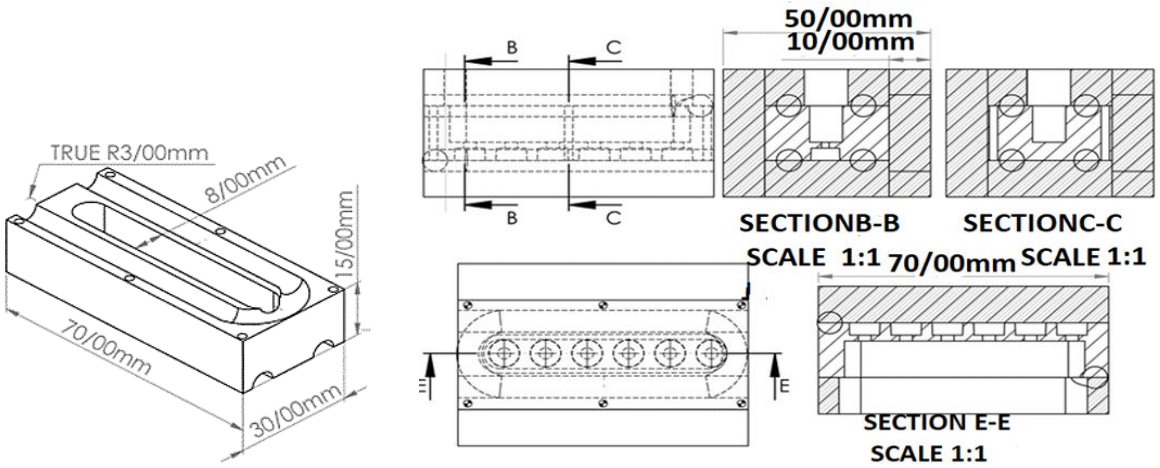

Fig. 4 Cross-Section of the Blade and Porous Media Retaining Piece

5. Flow Rate Adjustment: To explore different flow velocities, flow rates were adjusted using a control valve. Each adjustment led to the calculation of corresponding velocities.

6. Pressure Testing: Pressure measurements were taken under two distinct conditions: first, without installing the Porous Media piece, and second, after installing the Porous Media. These measurements were essential for understanding the impact of the Porous Media on pressure dynamics.

7. Numerical Analysis: In the numerical phase, particles were injected into the fluid flow. These particles had diameters ranging from 5 to 150 micrometers, with a total of 5 million particles. The analysis focused on pressure drops, sedimentation patterns, and deposition rates. The results obtained from this numerical analysis were meticulously documented.

8. Laboratory-Based Testing: The entire testing process was carried out exclusively within the laboratory environment.

9. Repeated Testing: It's important to note that all tests were conducted with a high degree of rigor, and the entire testing sequence was repeated twice to ensure consistency and reliability.

In summery the height of the water column in the barometric pressure section gave the pressure number, on the other hand, the flow rate was obtained by measuring the pump power. By having the diameter of the outlet pipe, we obtained the velocity, and through Bernoulli's equation, we obtained the pressure, and in this way, the analytical method of the read pressure was validated and this pressure became the basis of the numerical analysis.

For detailed information about the test conditions, including operational parameters, please refer to Table 2.

Table 2: General Test Conditions

Variable	Value measured	Unit
Ambient temperature	20	°C
Ambient pressure	899	hPa
The Input voltage to the pump	218	Volt
Pressure	315	mmH2O

4. UNCERTAINTY TEST

The evaluation of uncertainty about to the results of our tests, or calibration procedures, is a crucial aspect of ensuring the reliability and accuracy of our findings. This evaluation involves quantifying the uncertainties associated with various factors, as detailed in Table 3.

The standard of uncertainty is closely tied to the standard deviation of our measurements. This legal uncertainty is typically estimated as a range around a particular value. In our specific case, the legal uncertainty is defined as followed by Liu (2008):

$$u = \frac{a}{\sqrt{3}} \tag{1}$$

In the context of uncertainty assessment, it's essential to consider the standard character uncertainty and the precision of the measurement devices involved.

If we have a measurement device with a known accuracy, denoted as 'x,' and we are measuring a dimension 'y,' the actual value of 'y' can be considered to be within the range of 'y ± x'. In other words, the actual value of 'y' is expected to fall somewhere in this interval.

Now, when 'y' is a function of multiple inputs, say 'x_i,' the uncertainty in 'y' can be calculated as follows in Kirkup (2006).

$$U(y)_{=}\left[\left(\frac{\delta y}{\delta x_1}\right)^2 U^2(x_1)\left(\frac{\delta y}{\delta x_2}\right)^2 U^2(x_2)\ldots\right]^{\frac{1}{2}} \tag{2}$$

To calculate the uncertainty while considering the pump power, use the following equation:

$$P_{power} = V_{volt}.I_{current} \tag{3}$$

The uncertainty values for the variables, as listed in Table 3, can be incorporated into equation number 2 to ascertain the resulting uncertainty value in the following manner:

Table3 Measuring Instrument Uncertainties

Number	Equipment	Accuracy	Uncertainty
1.	Thermometers	0.01°C	0.005
2.	Multimeter	(1.1%+2) For 400μA/400mA±	0.006
		(0.9%+3) For100V/220V±	0.005
3.	Pressure column	0.2 mm	0.11

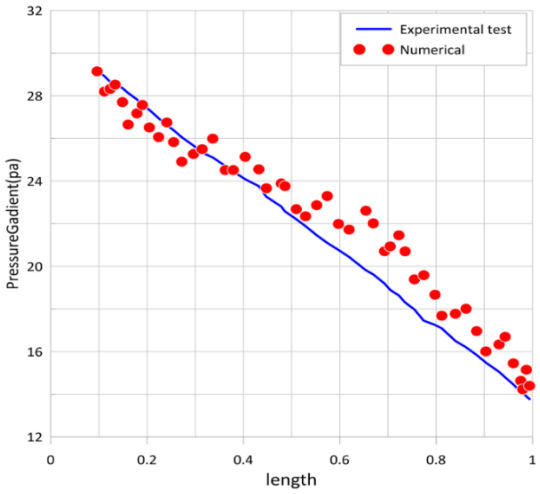

Fig. 5: Experimental and numerical validation

$$u_{(mult.)_=}\left[\left(\frac{\partial P}{\partial V_{volt}}\right)^2\left(u_{V_{volt}}\right)^2+\left(\frac{\partial P}{\partial I_{current}}\right)^2+\left(u_{I_{current}}\right)^2\right]^{\frac{1}{2}} \quad (4)$$

The values outlined in Table 3 represent independent parameters, while the outcomes of our analyses and calculations are reliant on these independent parameters. Equation No. 2 serves the purpose of computing the associated uncertainty and is commonly referred to as the compound uncertainty equation.

5. RESULTS

The experimental testing process was executed through various methodologies, acknowledging that the test approach can influence the results significantly. Therefore, it is imperative to validate the experimental test process. This validation was achieved through laboratory test validation using analytical solutions. Subsequently, the practical tests were cross-verified against numerical solutions for pressure gradients.

Figure 5, shows the numerical solution's validation of the pressure gradient and the experimental test. However, the graph shows a decrease in pressure. This phenomenon arises because the measured pressure is barometric, which essentially measures the total pressure. Consequently, the ambient pressure remains constant, and pressure drop along the tube's length is attributed to the fluid's internal conditions. In the other word while the fluid enters the tube, it experience more significant pressure losses. Conversely when the liquid reaches the end of the tube these losses diminish. Therefore, the graph exhibits a coherent correlation among numerical and experimental studies, the minor errors are relating the measurement and mesh analysis.

In Fig. 6, we visualize fluid velocity at two Reynolds numbers: 2930 and 8750. The Reynolds number serves as an indicator of the ratio between inertial forces and viscous forces, characterizing the fluid's movement. The

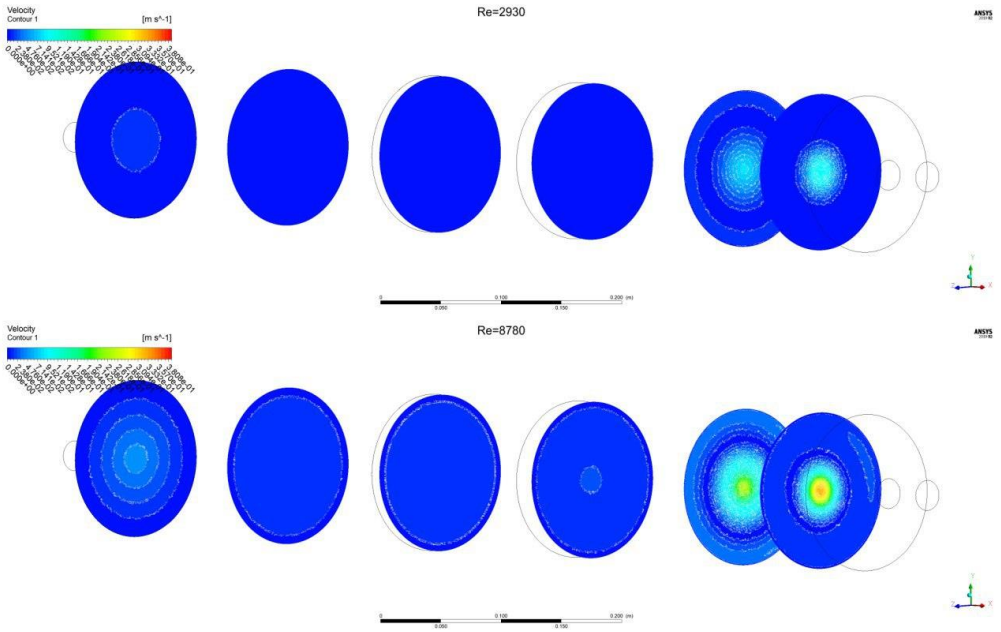

Fig. 6 Contour of velocity changes

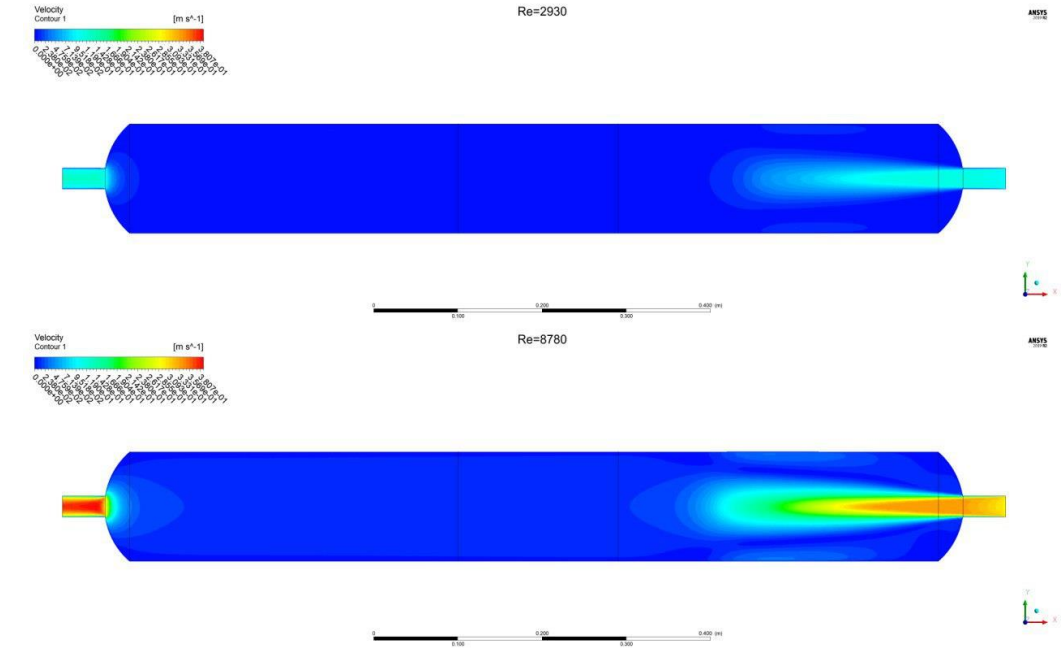

Fig. 7 Eddy viscosity variation along pipe length

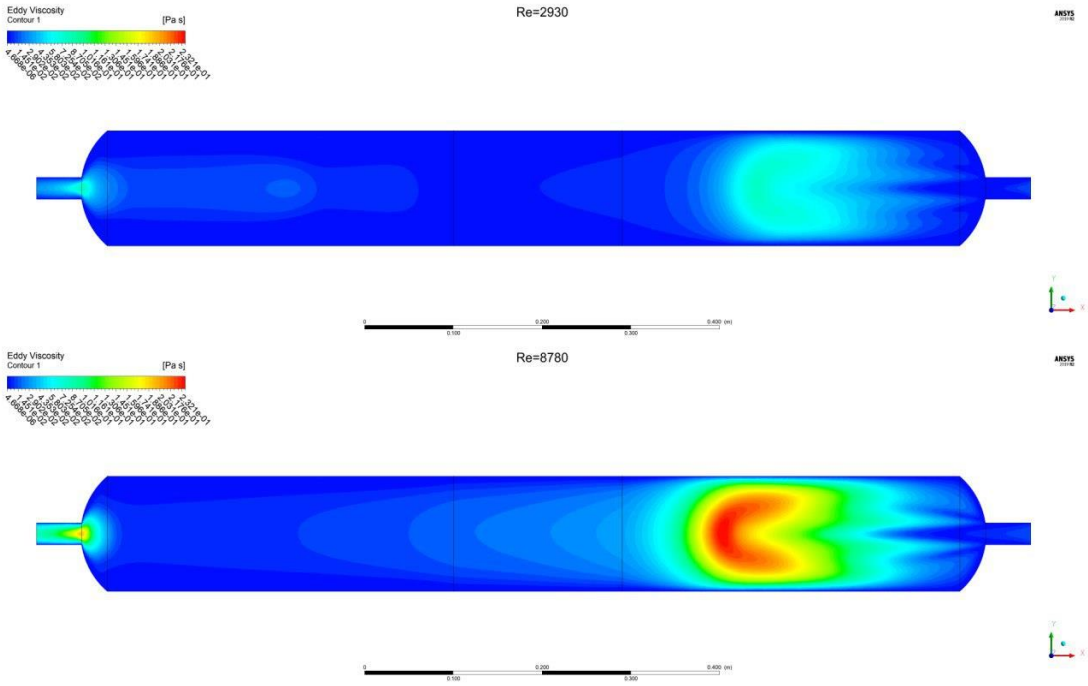

Fig. 8 Contour of velocity changes

turbulence or laminarity of the flow hinges on these forces, and these simulations offer an insightful representation of fluid behavior. We can observe the entry and exit of single-phase fluid in the sample pipe, which does not incorporate a porous medium. The Reynolds Number also provides a precise depiction of viscosity. As the diameter of the tube increases, it results in fluid retention within the line, ultimately affecting the point at which fluid exits due to elevated fluid rate. In incompressible fluid flow regimes, velocity and pressure are intricately linked, an issue that becomes apparent at the pipe's exit where the diameter decreases.

Figure 7 presents fluid velocity at Reynolds numbers 2930 and 8780 over 10 seconds. Eddy viscosity plays a crucial role as it serves as the proportional factor delineating turbulent energy transfer caused by the motion of eddies, giving rise to tangential stresses. This figure vividly illustrates the effects of velocity changes on fluid flow vortex formation.

Figure 8 depicts fluid flow vortices at Reynolds numbers 2930 and 8780. Changes in fluid velocity as the Reynolds number increases are evident in this diagram, illustrating the dynamic behavior of the fluid. The disparities in fluid behavior at the inlet and outlet lead to the formation of vortex flow patterns. The properties of the largest eddies are proportionate to those of the mean flow field, while the smallest eddies operate on a much larger timescale.

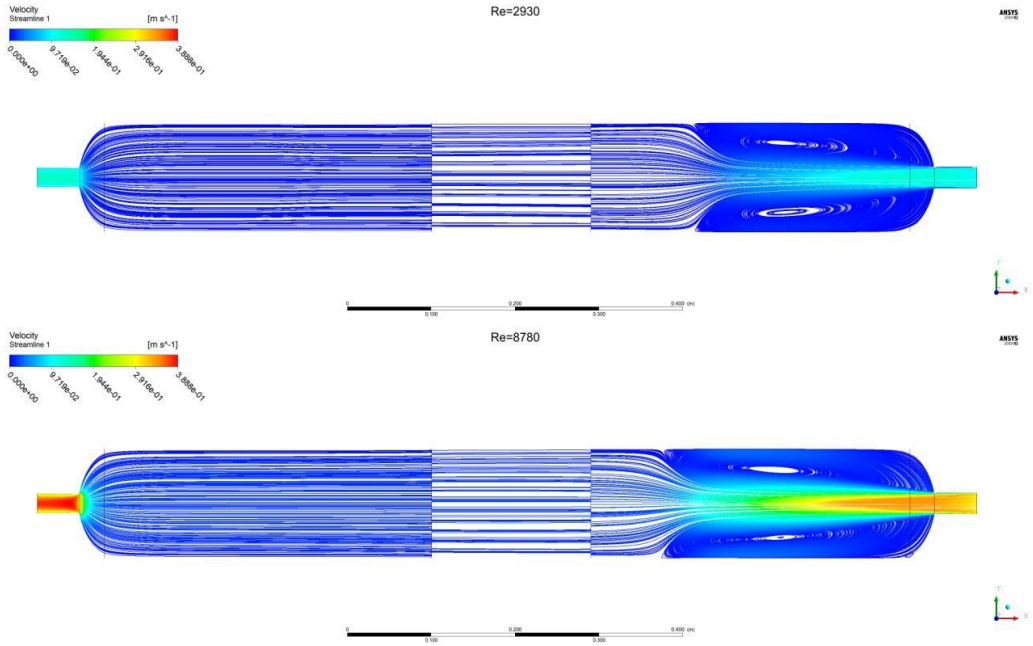

Fig. 9 Streamlines of fluid flow

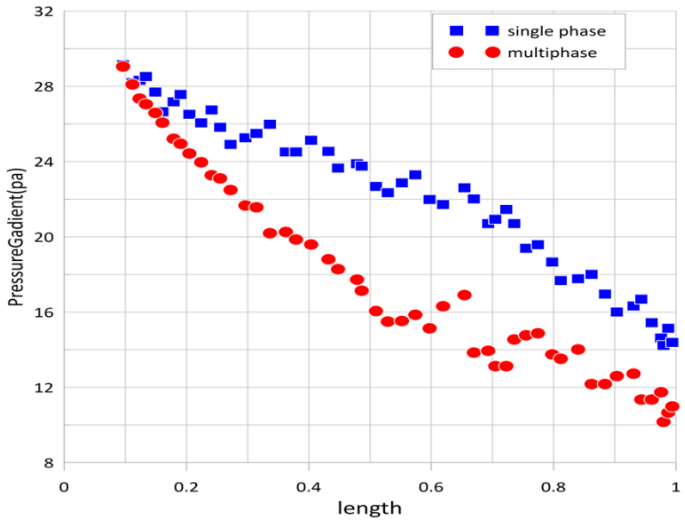

Fig. 10 Impact of Single-Phase and Two-Phase Fluids on Pressure Gradient

Figure 9 displays streamlines illustrating the behavior of single-phase fluid flow at Reynolds numbers 2930 and 8750. These lines trace the fluid velocity vectors tangent to the points. Flow lines do not intersect, as no flow crosses these lines. The shape of flow lines changes over time due to variations in velocity vectors. In steady flow, flow lines remain constant curves, except at singular points where speed is zero or infinite, leading to particle bifurcation.

Figure 10 illustrates changes in pressure gradient in single-phase and multiphase (two-phase) fluid flows. In multiphase fluid flow, momentum and energy equations interact, including fluid-particle, particle-particle, and fluid-fluid interfaces, leading to more excellent pressure resistance. Drag force significantly affects energy, resulting in a nonlinear graph for multiphase flow. In single-phase flow, the boundary layer thickness reaches 99% of the free stream value. In contrast, the boundary layer and particle interaction differ in multiphase flow, causing the graph to be nonlinear.

Figure 11 illustrates the pressure gradient in single-phase and multiphase fluid flow within porous media. In the porous medium, cross-section and boundary layer changes significantly increase vortices, altering the Reynolds number and causing a gap 5pa in the single phase and 8 pa in the multiphase pressure drop diagram. In multiphase fluid flow, interaction between liquid and particle, causing changes pressure gradient. The particle diameter ranges from 200 to 500 microns, the porosity diameter is one millimeter, however pressure drops. Velocity and pressure interactions play a pivotal role in fluid behavior. As shown in the figure the pressure gradient of multiphase fluid flow in Comparison of single phase remains constant after passing through porous media due to energy and exergy loss.

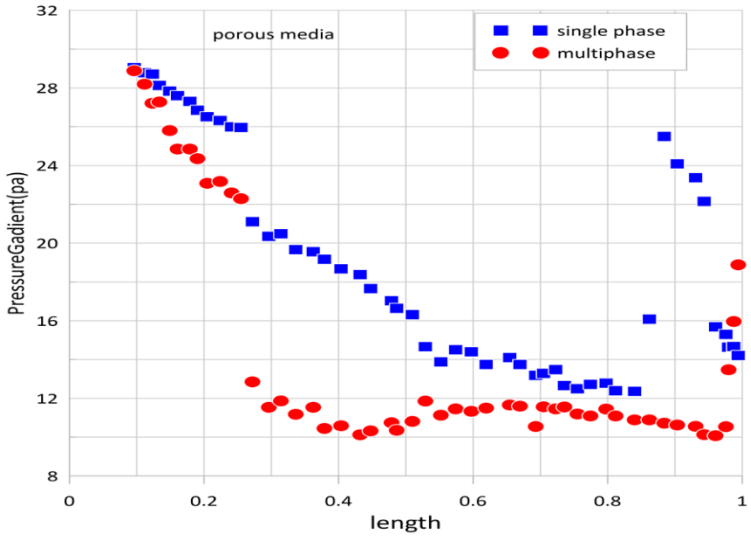

Fig. 11 Impact of single-phase and two-phase fluids on pressure gradient in porous media

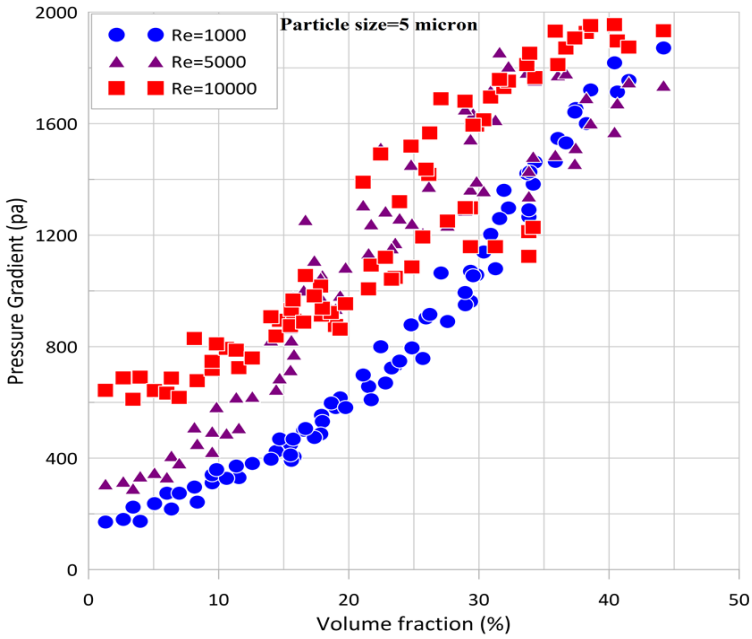

Fig. 12 Impact of Volume Fraction Percentage for 5-Micron Particle Size on Pressure Gradient

Figure 12 demonstrates the effect of volume fraction percentage on pressure gradient at different Reynolds numbers. As the volume fraction increases, indicating higher particle density and concentration, pressure drop escalates, necessitating more robust pumps. At a volume fraction of 40%, the curves nearly overlap. It's noteworthy that the precise point at which fluid behavior transitions to non-Newtonian is not clearly defined. It appears that beyond a 40% volume fraction, fluid flow tends toward non-Newtonian behavior. Pressure drop is a relative phenomenon influenced by numerous parameters, including loss rates, changes in cross-sectional area, density fluctuations, shocks, and alterations in momentum equations, all contributing to pressure drop. Figures 13 and 14 illustrate the impact of changes in particle diameter on pressure drop, with larger particle diameters demanding more energy due to increased energy losses and drag forces, resulting in higher pressure gradients.

Figure 15 demonstrates how alterations in volume fraction within the porous medium result in changes in the pressure gradient. Darcy's equation applies to single-phase fluid flows, whereas multiphase fluid flow in porous media demands distinct solutions. Solving the slope of momentum equations in the porous medium involves two steps: initially, Darcy's equation is employed, followed by a more general approach. Within the porous medium, particle and fluid equations solve simultaneously, considering momentum equations, energy equations, equations of state, interaction between fluid and solid, interaction between solid-solid, and correction equations for particles and liquid. This complex interplay leads to an increase in pressure gradient.

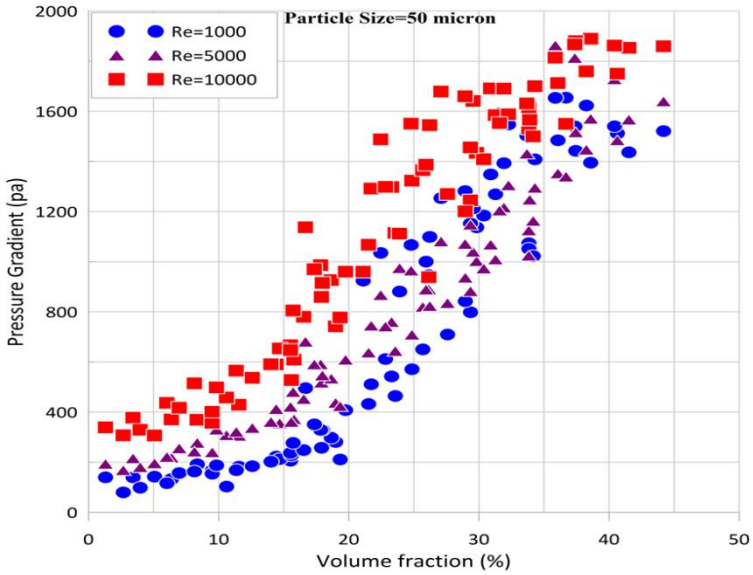

Fig. 13 Impact of Volume Fraction Percentage for 50-Micron Particle Size on Pressure Gradient

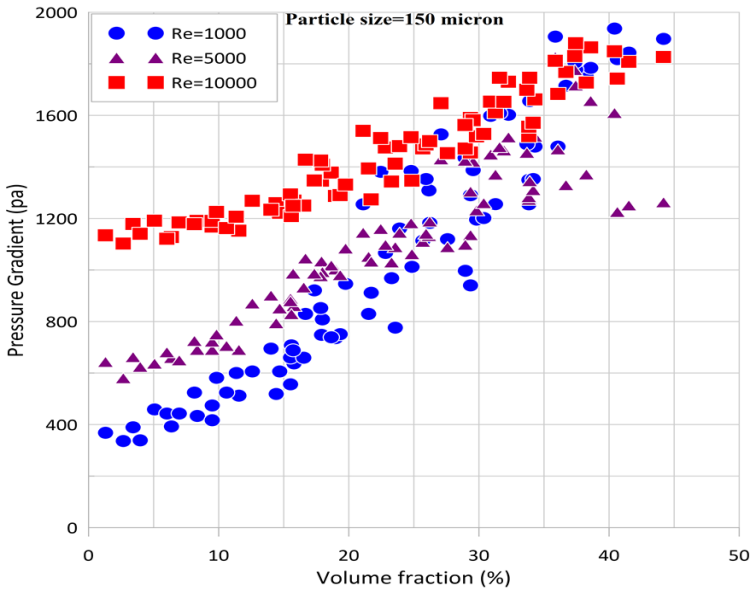

Fig. 14 Impact of Volume Fraction Percentage for 150-Micron Particle Size on Pressure Gradient

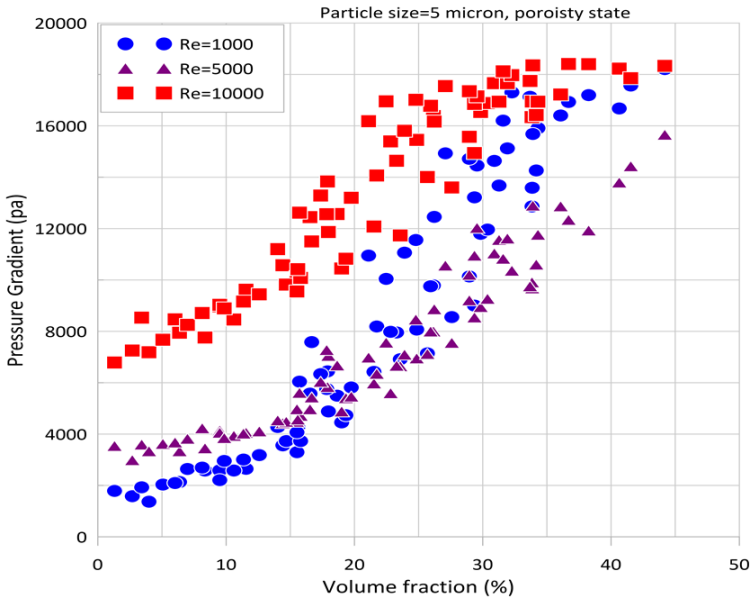

Fig. 15 Impact of Volume Fraction Percentage for 5-Micron Particle Size on Pressure Gradient in Porous Media

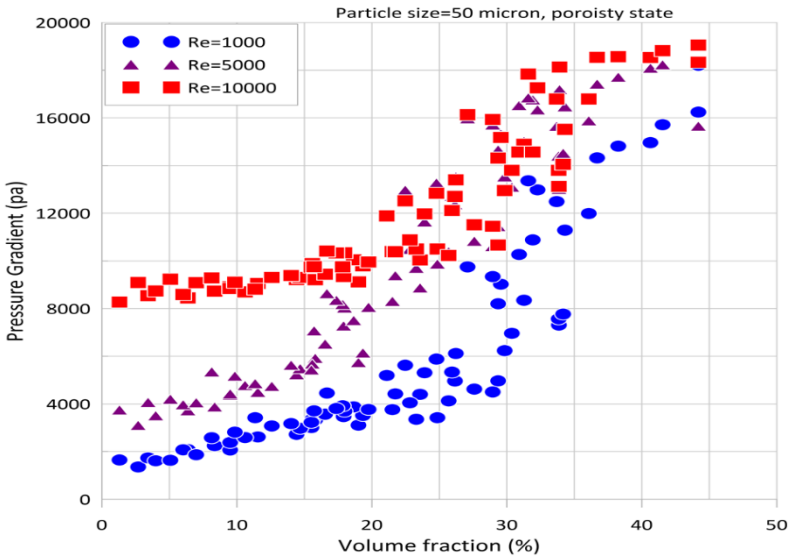

Fig. 16 Impact of Volume Fraction Percentage for 50-Micron Particle Size on Pressure Gradient in Porous Media

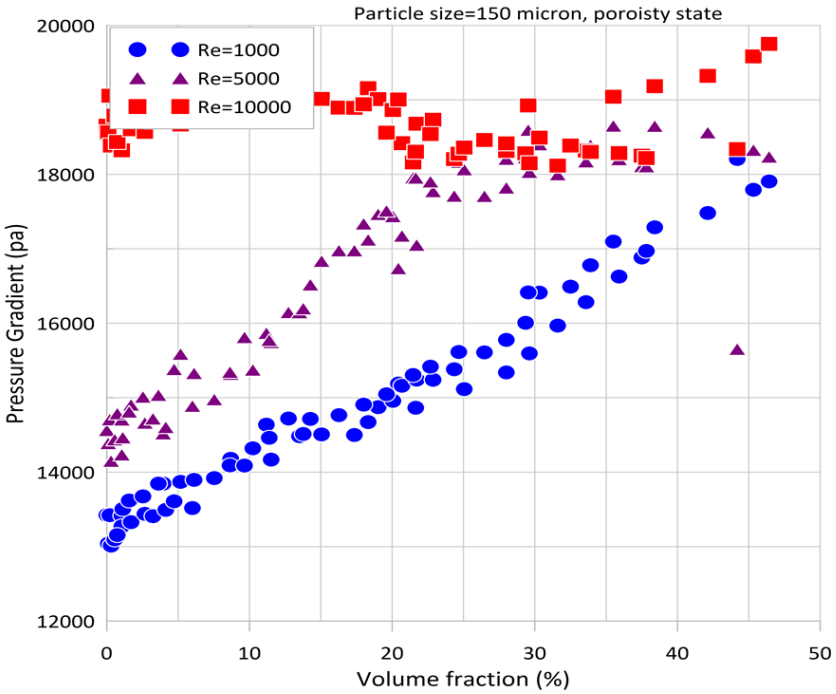

Fig. 17 Impact of Volume Fraction Percentage for 150-Micron Particle Size on Pressure Gradient in Porous Media

Figures 16 and 17 follow a similar theme to Figure 15 but emphasize the significance of particle diameter variations in influencing pressure drop. In Figure 17, the 150-micron diameter diagram reveals that, at Reynolds number 10,000, the pressure gradient remains constant due to porosity blockage**.**

Figure 18 explores how the porosity percentage influences the pressure gradient. It reveals that as porosity increases, fluid flow accelerates, leading to a decrease in pressure drop. Notably, the slopes in the graph vary significantly. There is a substantial difference in pitch between the Reynolds numbers of 1000 and 50,000. This discrepancy can be attributed to tabulated flows and the impact of the under-relaxation factor, acting as a correction factor that regulates the equations. The under-relaxation factor is crucial in mitigating fluctuations and distortions within the graph.

6. CONCLUSION

The pressure gradient is a complex phenomenon influenced by many factors including, energy loss rates, and changes in cross-sectional areas, density fluctuations, shocks, and variations in momentum equations. In the context of two-phase fluid flow within a porous medium, additional factors come into play. Interactions between solid particles with fluids, solid-solid interactions, and fluid interactions with the porous medium contribute to the pressure gradient. The size and nature of particles within the discrete phase, whether they are droplets or

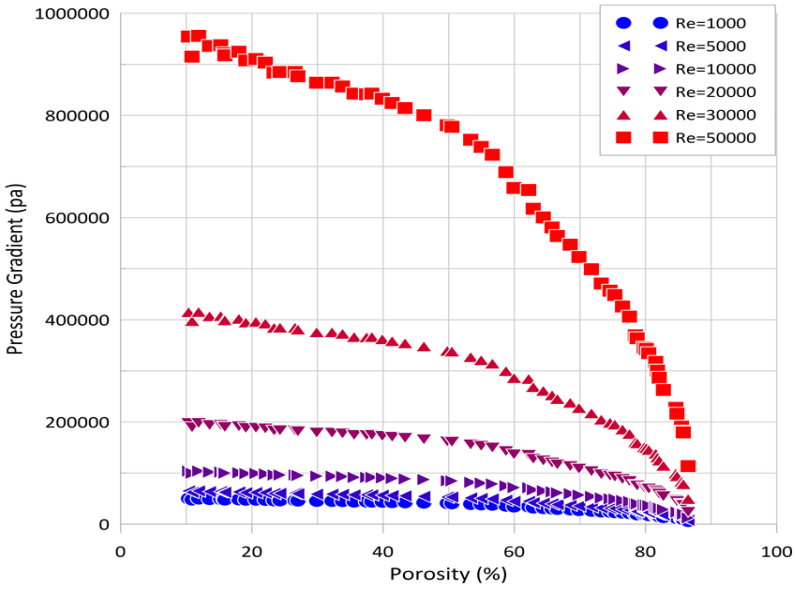

Fig. 18 Impact of Porosity Percentage Changes on Pressure Gradient

bubbles, significantly impact the range of the pressure gradient.

In this research, several key findings emerged:

1- Two-phase fluid flow in a porous medium exhibits a higher tolerance for pressure drop due to its interactions with the porous medium and the interplay between velocity and pressure. Additionally, it proves to be a suitable option for sediment formation.

2- The diameter of particles within porous media has a direct influence on the pressure drop. Larger particles possess greater mass, surface area, and momentum, leading to increased energy losses in fluid flow and, consequently, higher pressure gradients.

3- Porosity percentage plays a crucial role in determining the pressure gradient. As porosity increases, fluid flow becomes more efficient, reducing pressure drops.

4- Increasing the number of particles and their concentration within the fluid intensifies the pressure gradient. Pressure drop is inherently relative, and the graphs illustrate that higher volume fractions tend to lead to non-Newtonian behavior in the liquid.

5- . One of the calculating problems of the pressure drop is using the old methods for two-phase flow containing particles that follow the inability of the SIMPLE calculation algorithm to determine and detect the very low pressure gradient caused by the deposition of micro particles. In this research, by redefining the pressure calculation method based on the particles calculation and momentum changes Particles passing through the calculation unit cell, which is based on the changes in the particles velocity, it is possible to check the pressure drops on a small scale without considering the forces acting on the fluid and the solid on a micro scale.

These findings collectively shed light on the intricate dynamics of pressure gradients in two-phase fluid flow within porous media, offering valuable insights for applications across various industries and scientific fields.

CONFLICTS OF INTEREST:

The authors certify that they have NO affiliations with or involvement in any organization or entity with any financial interest (such as honoraria; educational grants; participation in speakers' bureaus; membership, employment, consultancies, stock ownership, or other equity interest; and expert testimony or patent-licensing arrangements), or non-financial interest (such as personal or professional relationships, affiliations, knowledge or beliefs) in the subject matter or materials discussed in this manuscript.

AUTHORS CONTRIBUTION:

H. Ashouri: Study concept and design, Analysis and interpretation of data, Drafting of the manuscript, Critical revision of the manuscript for important intellectual content; **H. Mohammadiun**: Study concept and design, Analysis and interpretation of data, supervision; **M. Mohammadiun**: Analysis and interpretation of data, supervision; **G. Shafiee Sabet**: Critical revision of the manuscript for important intellectual content; **M. H. Dibaee Bonab**: Statistical analysis; **F. Sabbaghzadeh**: Administrative, technical, and material support.

REFERENCES

Akram, S., Athar, M., Saeed, K., Razia, A., Alghamdi, M., & Muhammad, T. (2022). Impact of partial slip on double diffusion convection of sisko nanofluids in asymmetric channel with peristaltic propulsion and inclined magnetic field. *Nanomaterials, 12*(16), 2736. https://doi.org/10.3390/nano12162736

Alomar, O. R., Hamdoon, O. M., & Salim, B. M. (2020). Analysis of two-phase flow in a double-pipe heat

exchanger filled with porous media. *International Journal of Heat and Mass Transfer, 156*, 119799. https://doi.org/10.1016/j.ijheatmasstransfer.2020.119799

Arasteh, H., Mashayekhi, R., Ghaneifar, M., & Toghraie, D. (2019). Heat transfer enhancement in a counter-flow sinusoidal parallel-plate heat exchanger partially filled with porous media using metal foam in the channels' divergent sections. *Journal of Thermal Analysis and Calorimetry*, 1-17. https://doi.org/10.1007/s10973-019-08870-w

Bear, J. and M. Y. Corapcioglu (1948). *Fundamentals of transport phenomena in porous media*. M. Nijhoff. https://doi.org/10.1007/978-94-009-6175-3

Chen, S., & M. Krafczyk (2009) entropy generation in turbulent natural convection due to internal heat generation. *International Journal of Thermal Sciences, 48(*10), 1978-1987. https://doi.org/10.1016/j.ijthermalsci.2009.02.012

Chen, T. B. Y., Liu, L., Yuen, A. C. Y., Chen, Q., & Yeoh, G. H., (2023a). A multiphase approach for pyrolysis modelling of polymeric materials. *Experimental and Computational Multiphase Flow, 5*(2), 199-211. https://doi.org/10.1016/j.jaap.2020.104931

Chen, X., Li, Y., Liu, Z., & Zhang, J. (2023b). Experimental and theoretical investigation of the migration and plugging of the particle in porous media based on elastic properties. *Fuel, 332*, 126224. https://doi.org/10.1016/j.fuel.2022.126224

Hasanzadeh, Y., Alavi Fazel, S. A., & Azizi, Z. (2022). Experimental investigation on super high viscosity oil-water two-phase flow in a horizontal pipe. *Iranian Journal of Chemistry and Chemical Engineering*, *41*(2), 635-651. https://doi.org/10.30492/ijcce.2022.122737.4015

Janfada, T. S., Kasiri, N., & Dehghani, M. R. (2022). Modeling of direct contact condensation in the water-saturated zone of the soil exposed to steam injection. *Iranian Journal of Chemistry and Chemical Engineering*, *41*(3), 1003-1021. https://doi.org/10.30492/ijcce.2021.86714.3119

Jiang, Y., Li, Y., Ding, Y., Hu, S., Dang, J., Yang, F., & Ouyang, M., (2023). Simulation and experiment study on two-phase flow characteristics of proton exchange membrane electrolysis cell. *Journal of Power Sources, 553*, 232303. https://doi.org/10.1016/j.jpowsour.2022.232303

Joibary, S. M. M., & Siavashi, M. (2019). Effect of Reynolds asymmetry and use of porous media in the counterflow double-pipe heat exchanger for passive heat transfer enhancement. *Journal of Thermal Analysis and Calorimetry*, 1-15. https://doi.org/10.1007/s10973-019-08991-2

Kirkup, L. (2006). *An Introduction to Uncertainty in Measurement Using the Gum :(Guide to the Expression of Uncertainty in Measurement.* Cambridge University Press. https://doi.org/10.1017/CBO9780511755538

Liang, F., He, Z., Meng, J., Zhao, J., & Yu, C. (2023). Effects of microfracture parameters on adaptive pumping in fractured porous media: Pore-scale simulation. *Energy, 263*, 125950. https://doi.org/10.1016/j.energy.2022.125950

Liu, B. (2008). Fuzzy process, hybrid process and uncertain process. *Journal of Uncertain Systems, 2*(1), 3-16.

Man, Y., Tong, J., Wang, T., Wang, S., & Xu, H. (2023). Study on intermittent microwave convective drying characteristics and flow field of porous media food. *Energies, 16*(1), 441. https://doi.org/10.3390/en16010441

Mellouli, S., Dhaou, H., Askri, F., & Jemni, A. (2009). Hydrogen storage in metal hydride tanks equipped with metal foam heat exchanger. *International Journal of Hydrogen Energy, 34*(23), 9393-9401. https://doi.org/10.1016/j.ijhydene.2009.09.043

Naqvi, S. M. A., & Wang, Q. (2020). Performance enhancement of shell-tube heat exchanger by clamping anti-vibration baffles with porous media involvement. *Heat Transfer Engineering, (just-accepted*, 1-21. https://doi.org/10.1080/01457632.2020.1807098

Roman, S. (2023). How interfacial dynamics controls drainage pore-invasion patterns in porous media. *Advances in Water Resources, 171*, 104353. https://doi.org/10.1016/j.advwatres.2022.104353

Saeed, K., Akram, S., Ahmad, A., Athar, M., Razia, A., & Muhammad, T. (2022). Impact of slip boundaries on double diffusivity convection in an asymmetric channel with magneto-tangent hyperbolic nanofluid with peristaltic flow. *ZAMM-Journal of Applied Mathematics and Mechanics/Zeitschrift für Angewandte Mathematik und Mechanik, 103*(1), e202100338. https://doi.org/10.1016/j.csite.2021.100965

Sharma, V. K., Singh, A., & Tiwari, P. (2023). An experimental study of pore-scale flow dynamics and heavy oil recovery using low saline water and chemical flooding. *Fuel, 334*, 126756. https://doi.org/10.1016/j.fuel.2022.126756

Shirvan, K. M., Ellahi, R., Mirzakhanlari, S., & Mamourian, M. (2016). Enhancement of heat transfer and heat exchanger effectiveness in a double pipe heat exchanger filled with porous media: numerical simulation and sensitivity analysis of turbulent fluid flow. *Applied Thermal Engineering, 109*, 761-774. https://doi.org/10.1016/j.applthermaleng.2016.08.116

Siavashi, M., & Joibary, S. M. M. (2019). Numerical performance analysis of a counter-flow double-pipe heat exchanger with using nanofluid and both sides partly filled with porous media. *Journal of Thermal Analysis and Calorimetry, 135(2)*, 1595-1610. https://doi.org/10.1007/s10973-018-7829-z

Tammisola, O. (2023). Flow of yield-stress fluids through porous media. Science Talks, *5*, 100103.

https://doi.org/10.1016/j.sctalk.2022.100103

Tounsi, H., Rutqvist, J., Hu, M., & Wolters, R. (2023). Numerical investigation of heating and cooling-induced damage and brine migration in geologic rock salt: Insights from coupled THM modeling of a controlled block scale experiment. *Computers and Geotechnics*, *154*, 105161. https://doi.org/10.1016/j.compgeo.2022.105161

Zhang, X., & Tahmasebi, P. (2019). Effects of grain size on deformation in porous media. *Transport in Porous Media*, *129*(1), 321-341. https://doi.org/10.1007/s11242-019-01291-1

Zheng, C., Jun Guo, G., Qin, X., Dong, Y., Lu, C., Peng, B., Tang, W., & Bian, H. (2023). Molecular simulation studies on the water/methane two-phase flow in a cylindrical silica nanopore: Formation mechanisms of water lock and implications for gas hydrate exploitation. *Fuel*, *333*, 126258. https://doi.org/10.1016/j.fuel.2022.126258